Optical phonon spectrum and the Fröhlich Hamiltonian in würtzite-type nanotubes

2009 J. Phys.: Condens. Matter 21 485301

(http://iopscience.iop.org/0953-8984/21/48/485301)

IOP PUBLISHING JOURNAL OF PHYSICS: CONDENSED MATTER

J. Phys.: Condens. Matter **21** (2009) 485301 (9pp) doi:10.1088/0953-8984/21/48/485301

Optical phonon spectrum and the Fröhlich Hamiltonian in würtzite-type nanotubes

D E N Brancus and L Ion

Faculty of Physics, University of Bucharest, street Atomistilor no. 405, POB MG-11, 077125, Magurele-Ilfov, Romania

E-mail: dane@solid.fizica.unibuc.ro and lucian@solid.fizica.unibuc.ro

Received 17 August 2009, in final form 6 October 2009
Published 30 October 2009
Online at stacks.iop.org/JPhysCM/21/485301

Abstract

Dispersion laws of the full optical phonon spectrum of a nanotube made of würtzite-type materials as well as the corresponding Fröhlich electron–phonon interaction terms are derived and studied within the framework of the dielectric continuum model for a uniaxial crystal. The coupling coefficients describing electron–phonon interaction are obtained in an analytical closed form, depending on the dispersion law of the involved phonon branch. We present and discuss results of numerical calculations of optical phonon spectrum and Fröhlich coupling coefficients for some chosen würtzite AlN nanotubes. Observed features, induced by the anisotropy of würtzite-type materials, are discussed.

(Some figures in this article are in colour only in the electronic version)

1. Introduction

Since their discovery, initially as a particular form of carbon [1], nanotubes (NTs) have been subject to a thorough study, both theoretical, due to their fundamental significance, and experimental, due to their potential applications in various fields of technology. With the advent of new growth techniques, an increasing number of anisotropic würtzite-type materials, such as ZnO [2], GaN [3, 4], AlN [5, 6], BN [7], have been successfully cast in q-1D NTs.

For device applications, understanding the electron–phonon interactions in NTs is of great importance, particularly in the case of würtzite III-nitride semiconductors, where it is known that electron–optical phonon interaction plays a main role in determining free carrier mobility. The studies of the electron–optical phonon interaction (Fröhlich interaction) in nanostructures are based mainly on the dielectric continuum (DC) model [8]. One can identify two main reasons for using the DC model: first, it allows one to obtain analytical closed-form expressions that can be used for calculating the properties of nanostructures made of structurally similar materials, at least in the limit of long wavelength phonons. Secondly, this model is essentially analogous to the envelope-function method used for describing the electronic spectrum in nanostructures; consequently, on this basis, electron–phonon coupling can be consistently analyzed. In addition, it is worth mentioning that the results obtained with the DC model, e.g. in the case of GaAs/AlAs planar heterostructures, were proved to be in good agreement, within the limits of their validity, with those resulting from detailed microscopic calculations [9] or found in experiments [10].

Recently, the DC model was used to describe some features of optical phonon spectra and electron–optical phonon coupling in q-1D anisotropic (würtzite-type) semiconductor systems [11–13]. Those studies were mainly devoted to the interface phonon modes and their coupling with conduction band electrons in würtzite GaN/AlN cylindrical quantum wires [12] or core–shell würtzite cylindrical quantum wires [13]. Also, a classification of the possible types of optical phonon modes in q-1D nanostructures was proposed [12, 13]. The full spectrum of the optical phonons, as well as their interaction with electrons in a freestanding quantum wire made of würtzite-type materials and the corresponding polaron problem were investigated in [16].

The aim of this paper is to investigate confinement effects on optical phonons and on electron–optical phonon interaction in a cylindrical nanotube made of anisotropic, würtzite-type materials. It is organized as follows: the dielectric continuum model appropriate for use with our considered anisotropic system is introduced in section 2. We then calculate and analyze, in section 3, the full optical phonon spectrum of the nanotube; numerical results carried out in the case of würtzite AlN cylindrical NTs, for two different ratios of the inner and outer radii are presented and discussed. Finally, in section 4, the Fröhlich Hamiltonian is obtained; Fröhlich

coupling constants are calculated numerically and the results are discussed.

2. Equations of the model

We consider a cylindrical tube having inner radius R_1 and outer radius R_2, made of an uniaxial anisotropic polar material with its optical axis directed along the tube axis. To simplify the study of the optical phonon modes in such a system, we work in the context of the dielectric continuum (DC) model, restricting ourselves to the case of polar crystals having the optical phonon field described by a 3D real vector field. This assumption allows us to investigate the properties of optical phonons in uniaxial crystals such as layered materials (InSe, GaSe, PbI_2, etc), würtzite-type materials (ZnO, CdS, GaN, AlN, InN), and other anisotropic polar materials. However, the numerical results presented in this paper are restricted to the case of AlN. According to the uniaxial symmetry involved, the equations of the model are written in terms of three vector fields ($\vec{u}(\vec{r},t)$—the optical phonon field, $\vec{P}(\vec{r},t)$—the polarization field and $\vec{E}(\vec{r},t)$—the electric field) [14]:

$$\begin{aligned}\ddot{\vec{u}}_\alpha(\vec{r},t) &= \beta_{11}^\alpha \vec{u}_\alpha(\vec{r},t) + \beta_{12}^\alpha \vec{E}_\alpha(\vec{r},t)\\ \vec{P}_\alpha(\vec{r},t) &= \beta_{12}^\alpha \vec{u}_\alpha(\vec{r},t) + \beta_{22}^\alpha \vec{E}_\alpha(\vec{r},t)\end{aligned} \tag{1}$$

where the index α corresponds to a direction that is either parallel ($\alpha = \|$) or perpendicular ($\alpha = \perp$) to the optical axis. The expressions of the β-coefficients lead to a diagonal form for the dielectric tensor, with the components [14]:

$$\varepsilon_\alpha(\omega) = \varepsilon_\alpha(\infty)\frac{(\omega_{\mathrm{LO}}^\alpha)^2 - \omega^2}{(\omega_{\mathrm{TO}}^\alpha)^2 - \omega^2}, \tag{2}$$

where $\varepsilon_\alpha(\infty), \omega_{\mathrm{TO}}^\alpha$ and $\omega_{\mathrm{LO}}^\alpha$ are high frequency dielectric constant, the transverse phonon mode frequency and the longitudinal phonon mode frequency along the principal direction α, respectively. In the electrostatic approximation, the electrostatic potential $\Phi(\vec{r},t)$ is the key quantity of the problem. Performing a partial time-Fourier transform of the fields involved, the components of the phonon field are obtained from (1) in terms of the spatial derivatives of the electrostatic potential, according to the relation:

$$\sum_{\alpha=\|,\perp} g_\alpha(\omega)\vec{u}_\alpha(\vec{r},\omega) = -\nabla\Phi(\vec{r},\omega) \tag{3}$$

where

$$g_\alpha(\omega) = [(\omega_{\mathrm{TO}}^\alpha)^2 - \omega^2]/\beta_{12}^\alpha. \tag{4}$$

In every distinct domain of the system ($\rho < R_1, R_1 < \rho < R_2$, or $\rho > R_2$), the electrostatic potential satisfies the following equations:

$$\triangle\Phi^{(1)} = 0, \qquad (\rho < R_1) \tag{5}$$

$$\varepsilon_\|(\omega)\frac{\partial^2\Phi^{(2)}}{\partial x_3^2} + \varepsilon_\perp(\omega)\left(\frac{\partial^2\Phi^{(2)}}{\partial x_1^2} + \frac{\partial^2\Phi^{(2)}}{\partial x_2^2}\right) = 0, \quad (R_1 < \rho < R_2) \tag{6}$$

$$\triangle\Phi^{(3)} = 0, \qquad (\rho > R_2), \tag{7}$$

where $\rho = (x_1^2 + x_2^2)^{1/2}$.

In terms of cylindrical coordinates (ρ, z, φ), the electrostatic potential in domains 1 and 3 is given by the expressions:

$$\Phi^{(1)}(\rho,z,\varphi) = \sum_{\mathrm{m},q} a_{mq}^{(1)} W_{mq}(z,\varphi) I_{|m|}(|q|\rho), \tag{8}$$

$$\Phi^{(3)}(\rho,z,\varphi) = \sum_{\mathrm{m},q} a_{mq}^{(3)} W_{mq}(z,\varphi) K_{\mathrm{m}}(|q|\rho), \tag{9}$$

$I_{|m|}(z)$ and $K_{\mathrm{m}}(z)$ being the modified Bessel's functions of the first and the second kind, respectively [15]. By considering periodic boundary conditions along the optical axis of the system we obtain

$$W_{mq}(z,\varphi) = \frac{\mathrm{e}^{\mathrm{i}qz}\mathrm{e}^{\mathrm{i}m\varphi}}{\sqrt{2\pi L}}, \tag{10}$$

with $q = \frac{2\pi r}{L}$, $r = 0, \pm1, \pm2, \ldots$ and $m = 0, \pm1, \pm2, \ldots$, respectively; L is the length of the tube. In domain 2, the form of the electrostatic potential is

$$\Phi^{(2)}(\rho,z,\varphi) = \sum_{\mathrm{m},q}\left[a_{mq}^{(2)} f_{\mathrm{m}}^{(1)}\left(\frac{|q|\rho}{\sqrt{|s(\omega)|}}\right) + b_{mq}^{(2)} f_{\mathrm{m}}^{(2)}\left(\frac{|q|\rho}{\sqrt{|s(\omega)|}}\right)\right] W_{mq}(z,\varphi), \tag{11}$$

where, depending on the sign of the ratio $s(\omega) = \frac{\varepsilon_\perp(\omega)}{\varepsilon_\|(\omega)}$, the functions $f_{\mathrm{m}}^{(1)}(z)$ and $f_{\mathrm{m}}^{(2)}(z)$ are defined by the equalities: $f_{\mathrm{m}}^{(1)}(z) = I_{|m|}(z)$ and $f_{\mathrm{m}}^{(2)}(z) = K_{\mathrm{m}}(z)$ for $s > 0$ and, respectively, $f_{\mathrm{m}}^{(1)}(z) = J_{|m|}(z)$ and $f_{\mathrm{m}}^{(2)}(z) = Y_{|m|}(z)$ for $s < 0$; $J_{|m|}(z)$ and $Y_{|m|}(z)$ are Bessel's functions of the first and second kind. Standard electrostatic boundary conditions are considered at the two surfaces of the tube. At the surface $\rho = R_1$, these conditions lead to the equations:

$$I_{|m|}(|q|R_1) = \alpha_{mq}(\omega) f_{\mathrm{m}}^{(1)}\left(\frac{|q|R_1}{\sqrt{|s(\omega)|}}\right) + \beta_{mq}(\omega) f_{\mathrm{m}}^{(2)}\left(\frac{|q|R_1}{\sqrt{|s(\omega)|}}\right), \tag{12}$$

$$I'_{|m|}(|q|R_1) = \frac{\varepsilon_\perp(\omega)}{\sqrt{|s(\omega)|}}\left[\alpha_{mq}(\omega) f_{\mathrm{m}}^{(1)'}\left(\frac{|q|R_1}{\sqrt{|s(\omega)|}}\right) + \beta_{mq}(\omega) f_{\mathrm{m}}^{(2)'}\left(\frac{|q|R_1}{\sqrt{|s(\omega)|}}\right)\right], \tag{13}$$

where $\alpha_{mq}(\omega) = a_{mq}^{(2)}(\omega)/a_{mq}^{(1)}(\omega)$, and $\beta_{mq}(\omega) = b_{mq}^{(2)}(\omega)/a_{mq}^{(1)}(\omega)$. By introducing the quantity $\xi_1 = \frac{|q|R_1}{\sqrt{|s(\omega)|}}$ and taking into account the classical expression of the Wronskian of the solutions of Bessel's equation [15],

$$f_{\mathrm{m}}^{(1)'}(z) f_{\mathrm{m}}^{(2)}(z) - f_{\mathrm{m}}^{(1)}(z) f_{\mathrm{m}}^{(2)'}(z) = \frac{s(\omega)}{|s(\omega)|}\frac{1}{z}, \tag{14}$$

the expression of $\alpha_{mq}(\omega)$ and $\beta_{mq}(\omega)$ coefficients are obtained:

$$\alpha_{mq}(\omega) = -\xi_1\frac{s}{|s|}\left[I_{|m|}(|q|R_1) f_{\mathrm{m}}^{(2)'}(\xi_1) - \frac{\sqrt{|s(\omega)|}}{\varepsilon_\perp(\omega)} I'_{|m|}(|q|R_1) f_{\mathrm{m}}^{(2)}(\xi_1)\right], \tag{15}$$

$$\beta_{mq}(\omega) = \xi_1 \frac{s}{|s|}\left[I_{|m|}(|q|R_1) f_{\rm m}^{(1)'}(\xi_1) - \frac{\sqrt{|s(\omega)|}}{\varepsilon_\perp(\omega)} I'_{|m|}(|q|R_1) f_{\rm m}^{(1)}(\xi_1)\right]. \quad (16)$$

We have to note that the above defined $\alpha_{mq}(\omega)$ and $\beta_{mq}(\omega)$ coefficients depend on ω in two ways: firstly, through ξ_1 and, secondly, due to the presence of the factor $\frac{\sqrt{|s(\omega)|}}{\varepsilon_\perp(\omega)}$ in (15) and (16). Then, in domain 2, the electrostatic potential which, in addition, satisfies the electrostatic boundary conditions at the inner surface, has the form:

$$\Phi^{(2)}(\rho, z, \varphi) = \sum_{mq} a_{mq}^{(1)} F_{mq}(\xi, \omega) W_{mq}(z, \varphi), \quad (17)$$

where $\xi = \frac{|q|\rho}{\sqrt{|s(\omega)|}}$ and

$$F_{mq}(\xi, \omega) = \alpha_{mq}(\omega) f_{\rm m}^{(1)}(\xi) + \beta_{mq}(\omega) f_{\rm m}^{(2)}(\xi). \quad (18)$$

3. Optical phonon modes

By imposing electrostatic boundary conditions at the outer surface, $\rho = R_2$, ($\xi_2 = \frac{|q|R_2}{\sqrt{|s(\omega)|}}$), the equation for the dispersion law of the optical phonon modes can be written in the compact form:

$$f_{\rm m}(q, \omega) = 0, \quad (19)$$

where

$$f_{\rm m}(q, \omega) = -\frac{\sqrt{|s(\omega)|}}{\varepsilon_\perp(\omega)} \frac{F_{\rm m}(\xi_2, \omega)}{F'_{\rm m}(\xi_2, \omega)} + \frac{K_{\rm m}(|q|R_2)}{K'_{\rm m}(|q|R_2)}. \quad (20)$$

This way of writing the equation for the dispersion law of the optical phonon modes will be used in the appendix to obtain the normalization constant for the eigenvectors of the phonon field and, consequently, to put the electron–phonon interaction term into a closed form. In the following, in order to discuss the frequency spectrum of the optical phonon modes we use (15), (16), (18) and (20) to put (19) in its developed form:

$$\frac{f_{\rm m}^{(1)'}(\xi_1) - \frac{\sqrt{|s(\omega)|}}{\varepsilon_\perp(\omega)} f_{\rm m}^{(1)}(\xi_1) \frac{I'_{|m|}(|q|R_1)}{I_{|m|}(|q|R_1)}}{f_{\rm m}^{(1)'}(\xi_2) - \frac{\sqrt{|s(\omega)|}}{\varepsilon_\perp(\omega)} f_{\rm m}^{(1)}(\xi_2) \frac{K'_{\rm m}(|q|R_2)}{K_{\rm m}(|q|R_2)}} = \frac{f_{\rm m}^{(2)'}(\xi_1) - \frac{\sqrt{|s(\omega)|}}{\varepsilon_\perp(\omega)} f_{\rm m}^{(2)}(\xi_1) \frac{I'_{|m|}(|q|R_1)}{I_{|m|}(|q|R_1)}}{f_{\rm m}^{(2)'}(\xi_2) - \frac{\sqrt{|s(\omega)|}}{\varepsilon_\perp(\omega)} f_{\rm m}^{(2)}(\xi_2) \frac{K'_{\rm m}(|q|R_2)}{K_{\rm m}(|q|R_2)}}. \quad (21)$$

The classification of the optical phonon modes of the tube is similar to that used in the case of a wire [16], resulting in surface phonon modes for $s > 0$, with $\varepsilon_\perp < 0$, and confined phonon modes for $s < 0$ (quasilongitudinal modes for $\varepsilon_\perp < 0$ and quasitransverse modes for $\varepsilon_\parallel > 0$). The presence of the inner surface leads not only to the appearance of the corresponding surface phonon modes, but also to the modification, in the long wavelength range, of the whole phonon spectrum, as will be specified in the following.

3.1. Dispersion laws of surface phonon modes

The spectrum of the surface phonon modes, having frequencies distributed in the range $(\omega_{\rm TO}^{\perp}, \omega_{\rm LO}^{\parallel})$, is composed by two sets of phonon branches, each set corresponding to one surface. The phonon branches of the inner surface are situated in the upper part of the surface phonon spectrum. We introduce a new superscript index μ, taking the values 1 and 2 in order to label the surface phonon branches corresponding to the inner and outer surface, respectively. We shall call this index the character index and, in the following, we shall use it also to label the confined phonon modes (as quasitransverse phonon modes for $\mu = 3$ and quasilongitudinal phonon modes for $\mu = 4$). Among the surface phonon branches, the ones with the angular number $m = 0$ have a peculiar behavior, changing their character to a confined type at specific values of the wavevector $|q|$, irrespective of the value of the ratio R_1/R_2. Thus, by taking into account that in both situations $s(\omega) \to \infty$, for $\omega \to \omega_{\rm TO}^{\perp}, \omega > \omega_{\rm TO}^{\perp}$ in the case of the $m = 0$ branch of the outer surface modes ($\mu = 2$), or $\omega \to \omega_{\rm LO}^{\parallel}, \omega < \omega_{\rm LO}^{\parallel}$ in the case of the $m = 0$ branch of the inner surface modes ($\mu = 1$), respectively, approximate expressions of $m = 0$ Bessel's functions for small arguments ξ_1 and ξ_2 can be used, so that the value of $|q|$ which determines the branch character changing is obtained for each set. Then, the $m = 0$ phonon branch, corresponding to the outer surface, changes its character into that of the quasitransverse $m = 0$ branch, for values of $|q|$ smaller than $q_0^{(2)}$, given by

$$q_0^{(2)} = \frac{2}{R_2^2 - R_1^2} \frac{1}{\varepsilon_\parallel(\omega_{\rm TO}^{\perp})}\left[R_2 \frac{K'_0(q_0^{(2)}R_2)}{K_0(q_0^{(2)}R_2)} - R_1 \frac{I'_0(q_0^{(2)}R_2)}{I_0(q_0^{(2)}R_2)}\right]. \quad (22)$$

By taking the limit $R_1 \to 0$, the result obtained in the case of a quantum wire (see (33) in [16]) is recovered for $q_0^{(2)}$.

Also, the $m = 0$ phonon branch of the inner surface ($\mu = 1$) changes its character into that of the $m = 0$ quasilongitudinal phonon branch for $|q| < q_0^{(1)}$, where

$$q_0^{(1)} = \frac{\varepsilon_\perp(\omega_{\rm LO}^{\parallel})}{\ln\left(\frac{R_1}{R_2}\right)}\left[\frac{1}{R_1} \frac{I_0(q_0^{(1)}R_1)}{I'_0(q_0^{(1)}R_1)} - \frac{1}{R_2} \frac{K_0(q_0^{(1)}R_2)}{K'_0(q_0^{(1)}R_2)}\right]. \quad (23)$$

In the limit $|q| \to 0$, the phonon mode frequencies with $m \neq 0$ of the two sets depend on the ratio $\frac{R_1}{R_2}$, being given by the relation:

$$(\omega_{\rm m}^{(\mu)})^2 = \frac{(\omega_{\rm LO}^{\perp})^2 + (\omega_{\rm TO}^{\perp})^2 \frac{g_{\rm m}^{(\mu)}}{\varepsilon_\perp(\infty)}}{1 + \frac{g_{\rm m}^{(\mu)}}{\varepsilon_\perp(\infty)}}, \quad (24)$$

with $\mu = 1$ for the inner surface and $\mu = 2$ for the outer surface; we have denoted

$$g_{\rm m}^{(1)} = \frac{1 - \left(\frac{R_1}{R_2}\right)^m}{1 + \left(\frac{R_1}{R_2}\right)^m} = (g_{\rm m}^{(2)})^{-1}. \quad (25)$$

One can easily verify that, according to (24), the degeneracy of the surface modes with $m \neq 0$ at $q = 0$ encountered in the case of a wire (the common frequency value is the solution of the equation $\varepsilon_\perp(\omega) = -1$) [16] is lifted in the case of a tube. For the outer surface modes, irrespective of the ratio R_1/R_2, the

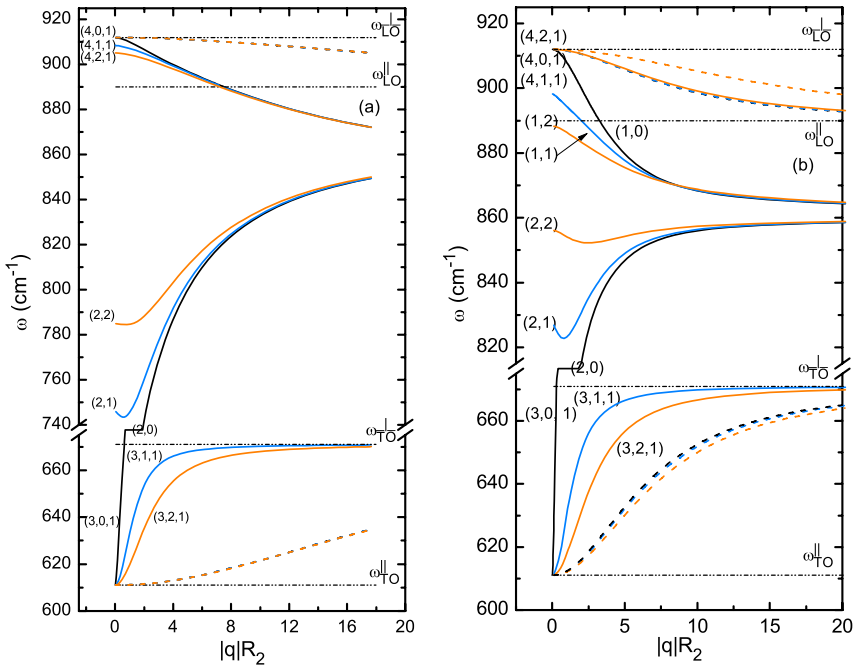

Figure 1. Spectrum of optical phonon modes of a würtzite-type AlN tube with $R_1/R_2 = 0.85$ (a) and $R_1/R_2 = 0.5$ (b), respectively. The phonon branches of all types with the same m value are drawn with the same type of line: a black line for $m = 0$, a blue (gray) line for $m = 1$ and an orange (light gray) line for $m = 2$. Solid lines with corresponding colors were used for drawing the modes with $l = 1$, while dashed lines were used for drawing the modes with $l = 2$. At the scale of the plot, both quasilongitudinal and quasitransverse confined modes with $l = 2$ are overlapping for $R_1/R_2 = 0.85$.

values (24) (in fact solutions of the equation $\varepsilon_\perp(\omega) = -g_{\rm m}^{(2)}$) always exist. However, the situation is quite different for the phonon modes of the inner surface, particularly in the domain of large wavelengths. Thus, an inner surface branch with $m \neq 0$ exists in the whole range of q only if the frequency $\omega_{\rm m}^{(1)}$, the solution of the equation $\varepsilon_\perp(\omega) = -g_{\rm m}^{(1)}$, is smaller than the value $\omega_{\rm LO}^{\parallel}$. Otherwise, at a specific value of $|q|$ denoted by $q_{\rm m}^{(1)}$, the branch adopts a quasilongitudinal-branch character. For $|q| \to \infty$, the branches of both sets meet the limit value ω_l, the inner branches from above and the outer branches from below, where ω_l is the corresponding solution of the equation $\varepsilon_\perp(\omega)\varepsilon_\parallel(\omega) = 1$.

3.2. Dispersion laws of confined phonon modes

The confined phonon modes of the tube, derived from the solutions of the electrostatic potential $\Phi^{(2)}(\rho, z, \varphi)$ for $s(\omega) < 0$, identified for a three-dimensional würtzite-type crystal with the so-called extraordinary optical phonon modes, can be classified, similar to the case of a wire [16], in quasilongitudinal modes, for $\omega \in (\omega_{\rm LO}^{\parallel}, \omega_{\rm LO}^{\perp})$, and quasitransverse modes, for $\omega \in (\omega_{\rm TO}^{\parallel}, \omega_{\rm TO}^{\perp})$. In addition to the indices m, q and μ, a supplemental index l appears, labeling different solutions of (21). Note that, in the case of a wire made of an isotropic material, this supplemental index is associated with the lth zero of the Bessel function $J_{|m|}(z)$.

For μ fixed, the phonon spectrum is composed by a set of confined phonon branches, $\omega = \omega_{mql}^{(\mu)} = \omega_{{\rm m}l}^{(\mu)}(q)$, depending on $|q|$. In the following, in order to be consistent with the notations used for treating in a similar manner the various types of phonon normal modes, we assign the index $l = 1$ for the surface modes ($\mu = 1, 2$) in the following notations $\omega_{mq1}^{(\mu)} = \omega_{{\rm m}1}^{(\mu)}(q) = \omega_{mq}^{(\mu)}$ and $\vec{u}_{mq1}^{(\mu)}(\vec{r}) = \vec{u}_{mq}^{(\mu)}(\vec{r})$. In figures 1(a) and (b), the full spectrum of optical phonon modes of an AlN tube is presented for the values 0.85 and 0.5 of the ratio R_1/R_2, respectively. The following values of AlN parameters were considered [17]: $\varepsilon_\parallel(\infty) = 4.77$, $\varepsilon_\perp(\infty) = 4.77$, $\omega_{\rm TO}^{\parallel} = 611\ {\rm cm}^{-1}$, $\omega_{\rm TO}^{\perp} = 671\ {\rm cm}^{-1}$, $\omega_{\rm LO}^{\parallel} = 890\ {\rm cm}^{-1}$ and $\omega_{\rm LO}^{\perp} = 912\ {\rm cm}^{-1}$. As can be seen, with increasing R_1/R_2 ratio, more quasilongitudinal ($\mu = 4$) phonon branches change their character into that of a inner surface ($\mu = 1$) phonon branch: (4, 0, 1), (4, 1, 1) and (4, 2, 1) in figure 1(a), and the branches (4, 0, 1) and (4, 1, 1) in figure 1(b). All other confined quasilongitudinal phonon branches start from $\omega_{\rm LO}^{\perp}$ for $|q|R_2 \to 0$ and go to $\omega_{\rm LO}^{\parallel}$ at large values of $|q|R_2$.

With regard to the quasitransverse phonon modes, all the branches start from $\omega_{\rm TO}^{\parallel}$, for small values of $|q|R_2$, and go to $\omega_{\rm TO}^{\perp}$, for large values of $|q|R_2$, excepting the branch with $m = 0$ which changes its character, becoming an outer surface branch for values of $|q|$ greater than $q_0^{(2)}$. Introducing the unit vectors $\{\vec{e}_\rho, \vec{e}_\varphi, \vec{e}_z\}$ of the cylindrical coordinates system, and considering (3), (4), and (17), the components of the phonon field eigenvectors (along, and perpendicular to the optical axis, respectively $\alpha = \parallel$ and $\alpha = \perp$) are given by the expressions:

$$\vec{u}_{mql,\parallel}^{(\mu)}(\rho, z, \varphi) = a_{mql}^{(\mu)(1)} \frac{{\rm i}q}{g_\parallel(\omega)} \vec{e}_z W_{mq}(z, \varphi) F_{\rm m}(\xi, \omega), \tag{26}$$

$$\vec{u}_{mql,\perp}^{(\mu)}(\rho, z, \varphi) = \frac{a_{mql}^{(\mu)(1)}}{g_\perp(\omega)} W_{mq}(z, \varphi) \times \left[\vec{e}_\rho \frac{|q|}{\sqrt{|s|}} F'_{\rm m}(\xi, \omega) + \vec{e}_\varphi \frac{{\rm i}m}{\rho} F_{\rm m}(\xi, \omega) \right], \tag{27}$$

where, in fact, the frequency ω is the frequency $\omega_{mql}^{(\mu)}$ of the corresponding normal mode. In a similar manner to that developed in appendix A of [16], the orthogonality relation verified by the eigenvectors of the optical phonon field is found:

$$\int_V \mathrm{d}v\, \vec{u}_{mql}^{(\mu)*}(\vec{r})\vec{u}_{m'q'l'}^{(\mu')}(\vec{r}) = \delta_{mm'}\delta_{qq'}\delta_{ll'}\delta_{\mu\mu'}. \tag{28}$$

Taking into account the orthogonality relation (28) and considering the above formulae, the expression of the normalization constant $a_{mql}^{(\mu)(1)}$ for all types of optical phonon modes is obtained, in the appendix, in the following compact form:

$$a_{mql}^{(\mu)(1)} = \frac{\left(\frac{2\omega_{mql}^{(\mu)}}{\varepsilon_0|q|R_2}\right)^{1/2}}{\left|\left[\varepsilon_\parallel(\omega)\varepsilon_\perp(\omega)\left(F'_{\mathrm{m}}\left(\frac{|q|R_2}{\sqrt{|s(\omega)|}}\right)\right)^2\frac{\partial f_{\mathrm{m}}(q,\omega)}{\partial\omega}\right]_{\omega=\omega_{mql}^{(\mu)}}\right|^{1/2}}. \tag{29}$$

3.3. Dispersion laws for a slab, obtained as a limiting case

Based on the asymptotic behavior of the Bessel functions at large arguments, $f_{\mathrm{m}}^{(1)}(\xi) \to (2\pi\xi)^{-1/2}e^{\xi}$ and $f_{\mathrm{m}}^{(2)}(\xi) \to (\frac{\pi}{2\xi})^{1/2}e^{-\xi}$ for $s > 0$, and, respectively, $f_{\mathrm{m}}^{(1)}(\xi) \to (\frac{2}{\pi\xi})^{1/2}\cos(\xi - \frac{\pi}{4} - \frac{m\pi}{2})$ and $f_{\mathrm{m}}^{(2)}(\xi) \to (\frac{2}{\pi\xi})^{1/2}\sin(\xi - \frac{\pi}{4} - \frac{m\pi}{2})$, for $s < 0$, in the limit $R_1, R_2 \to \infty$, but with $R_2 - R_1 = d = \text{const.}$, (21) recovers the form of the optical phonon dispersion law, with a wavevector directed along the optical axis, for an anisotropic slab having an optical axis in the plane of the slab:

$$\mathrm{e}^{-\frac{|q|d}{\sqrt{s}}} = p\frac{\varepsilon_\perp + \sqrt{s}}{\varepsilon - \sqrt{s}}, \qquad \text{for } s > 0, \tag{30}$$

and

$$\mathrm{e}^{-\mathrm{i}\frac{|q|d}{\sqrt{|s|}}} = p\frac{\varepsilon_\perp + \mathrm{i}\sqrt{|s|}}{\varepsilon - \mathrm{i}\sqrt{|s|}}, \qquad \text{for } s < 0, \tag{31}$$

p being the parity index, with $p = 1$ for symmetric modes and $p = -1$ for anti-symmetric modes.

4. Free phonon Hamiltonian and electron–phonon interaction

In this section, by paying an equal consideration to all types of optical phonons, the Fröhlich Hamiltonian is obtained for our considered anisotropic tube. First, we discuss the Hamiltonian of the free phonons. The Hamiltonian of the free optical phonons of a quantum wire H_{ph} was obtained in [16] by starting with the following expression for the energy density of the free optical phonons:

$$h(\vec{r}) = \sum_{\alpha=\parallel,\perp}\tfrac{1}{2}[\Pi_\alpha^2(\vec{r}) + (\omega_{\mathrm{TO}}^\alpha)^2u_\alpha^2(\vec{r}) - \beta_{12}^\alpha E_\alpha(\vec{r})u_\alpha(\vec{r})] \tag{32}$$

resulting in

$$H_{\mathrm{ph}} = \int_V \mathrm{d}v\, h(\vec{r}). \tag{33}$$

In (32), Π_α is the α-component of the momentum density, canonically conjugated to the corresponding component of the field u_α.

Here, in order to obtain the contributions of all types of phonons to H_{ph}, all the fields appearing into the forms of the Hamiltonian densities will be developed in terms of the eigenvectors of the phonon field, which verify the orthogonality relation (28). In the following, we shall consider $\vec{\Pi}(\vec{r})$ and $\vec{u}(\vec{r})$ as field operators written in the Schrödinger picture. Thus, the operator $\vec{u}(\vec{r})$ can be written in terms of the phonon normal modes (m, q, l, μ):

$$\vec{u}(\vec{r}) = \sum_{mql\mu}\lambda_{mql}^{(\mu)}[\vec{u}_{mql}^{(\mu)}(\vec{r})a_{mql}^{(\mu)} + \text{h.c.}], \tag{34}$$

where, without losing the generality of the problem, the quantities $\lambda_{mql}^{(\mu)}$ are considered to be real quantities, depending on $|m|$ and $|q|$; $a_{mql}^{(\mu)}$ and $a_{mql}^{(\mu)+}$ are the annihilation and creation operators for the phonon mode (m, q, l, μ). The operators $a_{mql}^{(\mu)}$ and $a_{mql}^{(\mu)+}$ satisfy typical Bose commutation relations:

$$\begin{gathered}[a_{mql}^{(\mu)}, a_{m'q'l'}^{(\mu')}] = 0, \qquad [a_{mql}^{(\mu)+}, a_{m'q'l'}^{(\mu')+}] = 0,\\ [a_{mql}^{(\mu)}, a_{m'q'l'}^{(\mu')+}] = \delta_{mm'}\delta_{ll'}\delta_{qq'}\delta_{\mu\mu'}.\end{gathered} \tag{35}$$

For the purpose of putting the phonon Hamiltonian into the form

$$H_{\mathrm{ph}} = \sum_{mql\mu}\hbar\omega_{\mathrm{ml}}^{(\mu)}(q)(a_{mql}^{(\mu)+}a_{mql}^{(\mu)} + \tfrac{1}{2}), \tag{36}$$

we make use of the classical equation of motion (formally identical with the equation verified by the operator written in the Heisenberg picture)

$$\vec{\Pi} = \dot{\vec{u}}, \tag{37}$$

to derive the following expression in the Schrödinger picture for the operator $\vec{\Pi}$:

$$\vec{\Pi}(\vec{r}) = -\mathrm{i}\sum_{mql\mu}\lambda_{mql}^{(\mu)}\omega_{\mathrm{ml}}^{(\mu)}(q)(\vec{u}_{mql}^{(\mu)}(\vec{r})a_{mql}^{(\mu)} - \text{h.c.}). \tag{38}$$

By using expression (34) of the operator $\vec{u}(\vec{r})$, the α component of the electric field operator in (1) can be put into the form:

$$E_\alpha(\vec{r}) = \sum_{mql\mu}\lambda_{mql}^{(\mu)}\frac{(\omega_{\mathrm{TO}}^\alpha)^2 - (\omega_{\mathrm{ml}}^{(\mu)}(q))^2}{\beta_{12}^\alpha}[(\vec{u}_{mql}^{(\mu)}(\vec{r}))_\alpha a_{mql}^{(\mu)} + \text{h.c.}], \tag{39}$$

with $\alpha = \parallel, \perp$. By using (32), (34), (38) and (39), and taking into consideration, in addition to the orthogonality relation (28), the relationship verified by the phonon normal modes

$$\vec{u}_{mql}^{(j)(\mu)*}(\vec{r}) = \vec{u}_{-m,-q,l}^{(j)(\mu)}(\vec{r}), \tag{40}$$

the desired form (36) of the Hamiltonian of optical phonons is obtained by choosing

$$\lambda_{mql}^{(\mu)} = \left(\frac{\hbar}{2\omega_{\mathrm{ml}}^{(\mu)}(q)}\right)^{1/2}. \tag{41}$$

Next, we derive the Hamiltonian describing the interaction of conduction band electrons and the optical phonon field (Fröhlich interaction). This interaction, induced by both types of polarization charges contributing to the electrostatic potential—the volume charges and the surface charges, is written as

$$H_{\mathrm{e-ph}} = e\Phi(\vec{r}), \qquad e < 0; \tag{42}$$

e is the electron charge and $\Phi(\vec{r})$ is the electrostatic potential including all of the above specified contributions.

Phonon mode contributions to this Hamiltonian will be obtained by developing the electrostatic potential in terms of eigenvectors of the phonon field. By taking into account the solution (11) for the electrostatic potential, the development (34) of the phonon vector field and the expression (41) of the constant $\lambda^{(\mu)}_{mql}$, the electron–phonon interaction Hamiltonian is obtained in the form:

$$H_{\mathrm{e-ph}} = -\sum_{mql\mu} \Gamma^{(\mu)}_{\mathrm{m}l}(q) \times \left[W_{mq}(z,\varphi) F_{\mathrm{m}} \left(\frac{|q|\rho}{\sqrt{|s(\omega^{(\mu)}_{\mathrm{m}l}(q))|}} \right) a^{(\mu)}_{mql} + \mathrm{h.c.} \right], \tag{43}$$

where

$$\Gamma^{(\mu)}_{\mathrm{m}l}(q) = \frac{(\frac{\hbar e^2}{\varepsilon_0 |q| R_2})^{1/2}}{\left| \left[\varepsilon_{\parallel}(\omega)\varepsilon_{\perp}(\omega) \left(F'_{\mathrm{m}} \left(\frac{|q|R_2}{\sqrt{|s(\omega)|}} \right) \right)^2 \frac{\partial f_{\mathrm{m}}(q,\omega)}{\partial \omega} \right]_{\omega=\omega^{(\mu)}_{mql}} \right|^{1/2}}. \tag{44}$$

Figures 2 and 3 show the behavior of the coupling coefficients $\Gamma^{(\mu)}_{\mathrm{m}l}(q)$ for all types of optical phonon modes for an AlN tube with $R_1/R_2 = 0.85$ and $R_1/R_2 = 0.5$, respectively; the coupling coefficients with $|m| \leqslant 2$ and $l = 1, 2$ are plotted in all cases ($\mu = 1, 2, 3, 4$). A significant result, also seen in the case of a quantum wire made of anisotropic materials [16], is that quasitransverse phonon modes interact with band conduction electrons. This is a consequence of the anisotropy of the material: for isotropic materials, coupling coefficients corresponding to transverse phonon modes are all zero. However, the values of $\Gamma^{(3)}_{\mathrm{m}l}(q)$ for quasitransverse modes are much less than their counterparts for quasilongitudinal ($\mu = 4$), inner ($\mu = 1$) or outer ($\mu = 2$) surface modes over the whole investigated $|q|R_2$ range. All the coupling coefficients corresponding to phonon modes whose character is changing from an (inner or outer) surface mode to a confined mode (quasitransverse or quasilongitudinal) are continuous, with continuous derivative at $|q|R_2$ values where this change occurs. An interesting observation is that, with increasing R_1/R_2 ratio, the values of $\Gamma^{(4)}_{\mathrm{m}l}(q)$ for quasilongitudinal modes, changing their character into inner surface modes, increase significantly at small $|q|R_2$ values.

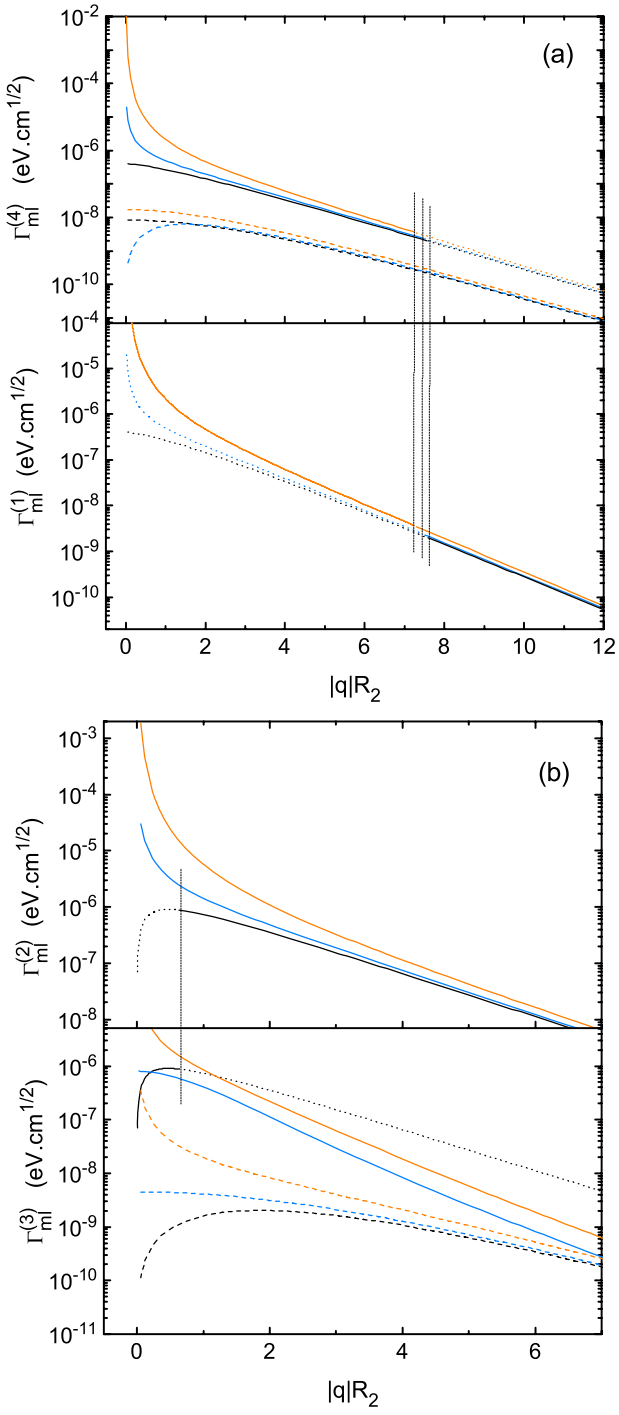

Figure 2. Coupling constants $\Gamma^{(1)}_{\mathrm{m}l}(q)$ and $\Gamma^{(4)}_{\mathrm{m}l}(q)$ (a) and, respectively, $\Gamma^{(2)}_{\mathrm{m}l}(q)$ and $\Gamma^{(3)}_{\mathrm{m}l}(q)$ (b) for a würtzite-type AlN tube with $R_1/R_2 = 0.85$. The values of $|q|R_2$ where the character is changing from a confined mode to a surface mode are marked by vertical dash-dotted lines. Coupling constants are plotted, respectively, in black for $m = 0$, in blue (gray) for $m = 1$ and in orange (light gray) for $m = 2$; solid lines correspond to $l = 1$, while dashed lines correspond to $l = 2$. Beyond the transition points where the change of character occurs, solid lines are continued with dotted lines, to illustrate the continuity of the corresponding $\Gamma^{(\mu)}_{\mathrm{m}l}(q)$s.

5. Summary

To summarize, dispersion laws of the full optical phonon spectrum for a cylindrical nanotube made of uniaxial anisotropic würtzite-type materials were obtained in the frame of the DC model. Using an appropriate form [16] of the energy density of the optical phonon system and the orthogonality relation verified by the eigenvectors of the optical phonon field, the contributions to the Hamiltonian of the system of all types of optical phonons were found. The presence of

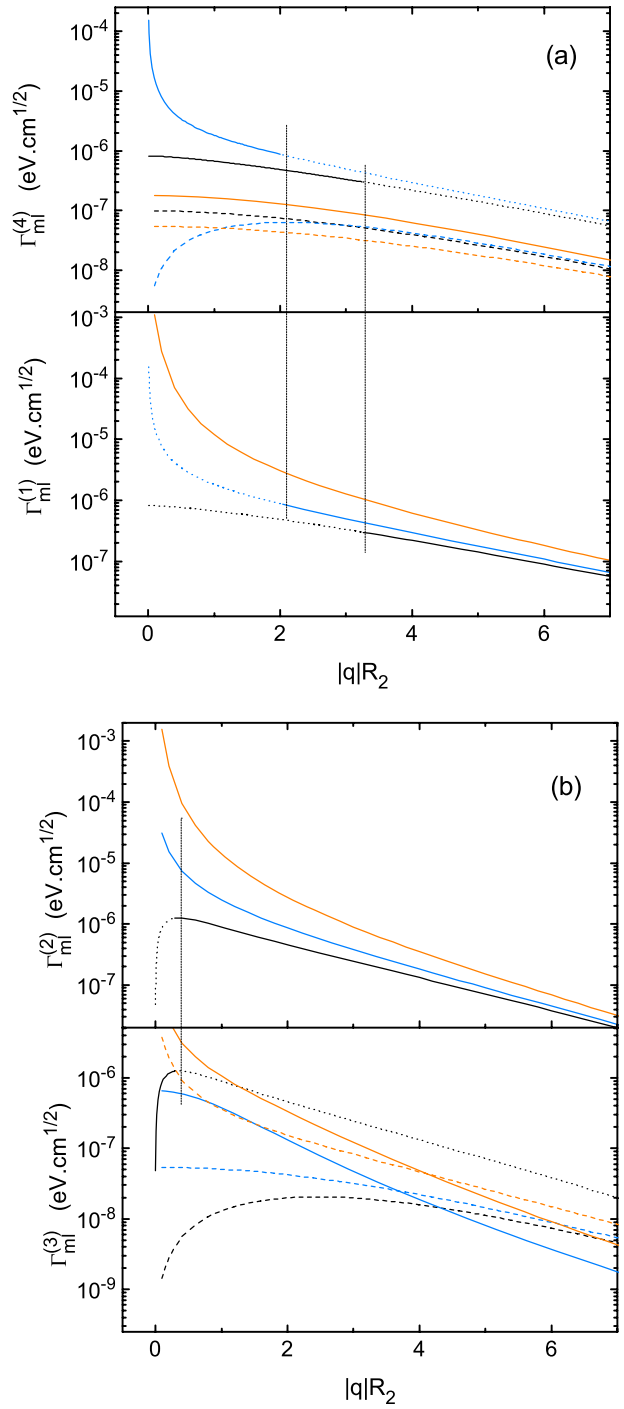

Figure 3. Coupling constants $\Gamma^{(1)}_{ml}(q)$ and $\Gamma^{(4)}_{ml}(q)$ (a) and, respectively, $\Gamma^{(2)}_{ml}(q)$ and $\Gamma^{(3)}_{ml}(q)$ (b) for a würtzite-type AlN tube with $R_1/R_2 = 0.5$. The values of $|q|R_2$ where the character is changing from a confined mode to a surface mode are marked by vertical dash-dotted lines. Coupling constants are plotted, respectively, in black for $m = 0$, in blue (gray) for $m = 1$ and in orange (light gray) for $m = 2$; solid lines correspond to $l = 1$, while dashed lines correspond to $l = 2$. Beyond the transition points where the change of character occurs, solid lines are continued with dotted lines, to illustrate the continuity of the corresponding $\Gamma^{(\mu)}_{ml}(q)$s.

the inner surface induces, in addition to the occurrence of the corresponding surface phonon modes, important modifications of the whole phonon spectrum in the long wavelength range. Thus, the degeneracy of the outer surface modes with $m \neq 0$ and $q \to 0$, encountered in the case of a wire [16], is raised in the case of the tube. Results of numerical calculations for nanotubes made of würtzite AlN were presented. As a consequence of the uniaxial anisotropy of the materials, all the confined modes show dispersion, in the range $[\omega^{\parallel}_{TO}, \omega^{\perp}_{TO}]$ in the case of quasitransverse modes and, respectively, in the range $[\omega^{\parallel}_{LO}, \omega^{\perp}_{LO}]$ in the case of quasilongitudinal modes. It was found that confined modes with angular number $m = 0$, both quasitransverse and quasilongitudinal, switch their character into that of a surface branch at specific values of the wavevector; this holds irrespective of the value of the ratio R_1/R_2. The $m = 0$ quasitransverse mode switch to $m = 0$ mode corresponding to the outer surface, while $m = 0$ quasilongitudinal mode switches to a $m = 0$ mode corresponding to the inner surface. In addition, depending on the R_1/R_2 value, $m \neq 0, l = 1$ quasilongitudinal branches may switch to inner surface branches with the same m: the greater the ratio R_1/R_2, the more pronounced this effect is. Also, the form of the interaction Hamiltonian of optical phonons with a conduction band electron was found. The coupling coefficients, describing the electron–optical phonon interaction, for all types of phonons, were obtained in an analytical closed form, which is an extension to this case of other similar expressions obtained for 3D [18] and q-2D [19] systems or q-1D nanowires [16] made of uniaxial anisotropic materials. As an effect of anisotropy, there is an interaction between quasitransverse phonon modes and conduction band electrons. However, this interaction is weaker than in the case of quasilongitudinal or surface phonon modes. For those phonon modes which switch from a quasitransverse or quasilongitudinal confined character to surface modes, the coupling coefficients are continuous with continuous derivative at the switching points. The results we have obtained are of practical interest in considering the polaron problem or the electron scattering on optical phonons in such type of systems, as well as in considering the problem of a q-1D axially-symmetric heterostructure of the type anisotropic material(1)/anisotropic material(2).

Acknowledgment

This work was supported by the National Authority for Scientific Research of Romania, under Grant no. PN II ID_1900.

Appendix

Considering (26) and (27) giving the components of the eigenvectors of the optical phonon field, the orthogonality relation (28) leads to the following expression of the normalization constant $a^{(1)}_{mq}$:

$$\left|a^{(1)}_{mq}\right|^{-2} = \int_{R_1}^{R_2} \mathrm{d}\rho\, \rho \left\{ \frac{q^2}{g^2_{\parallel}(\omega)} F^2_{\mathrm{m}}(\xi, \omega) + \frac{1}{g^2_{\perp}(\omega)} \left[\frac{m^2}{\rho^2} F^2_{\mathrm{m}}(\xi, \omega) + \frac{q^2}{|s|} (F'_{\mathrm{m}}(\xi, \omega))^2 \right] \right\}. \quad \text{(A.1)}$$

In the following, in order to simplify the expressions, we shall make the notation $\lambda = \frac{|q|}{\sqrt{|s|}}$, renouncing also, for the moment, to explicitly specify into the formulae the ω dependence of the different quantities: $F_{\rm m}(\lambda\rho, \omega)$, $s(\omega)$, $g_{\parallel,\perp}(\omega)$, $\varepsilon_{\parallel,\perp}(\omega)$. Now, integrating by parts the last term in the right-hand side of (A.1),

$$\int_{R_1}^{R_2} {\rm d}\rho\, \rho (F'_{\rm m}(\lambda\rho))^2 = \frac{\rho}{\lambda} F_{\rm m}(\lambda\rho) F'_{\rm m}(\lambda\rho)\Big|_{R_1}^{R_2} - \int_{R_1}^{R_2} {\rm d}\rho\, \rho F_{\rm m}(\lambda\rho)\left[F''_{\rm m}(\lambda\rho) + \frac{1}{\lambda\rho} F'_{\rm m}(\lambda\rho)\right], \tag{A.2}$$

and, taking into account the Bessel-type equation,

$$F''_{\rm m}(\lambda\rho) + \frac{1}{\lambda\rho} F'_{\rm m}(\lambda\rho) = \left(\frac{s}{|s|} + \frac{m^2}{\lambda^2\rho^2}\right) F_{\rm m}(\lambda\rho), \tag{A.3}$$

(A.1) becomes

$$|a_{mq}^{(1)}|^{-2} = \frac{\lambda\rho}{g_\perp^2} F_{\rm m}(\lambda\rho) F'_{\rm m}(\lambda\rho)\Big|_{R_1}^{R_2} + \left[\frac{q^2}{g_\parallel^2} - \frac{\lambda^2}{g_\perp^2}\frac{s}{|s|}\right] \int_{R_1}^{R_2} {\rm d}\rho\, \rho (F_{\rm m}(\lambda\rho))^2. \tag{A.4}$$

The last integral is an extension of the so-called Lommel-type integral [15] to the case of a general solution of the Bessel's equation (A.3). One obtains

$$\int_{R_1}^{R_2} {\rm d}\rho\, \rho (F_{\rm m}(\lambda\rho))^2 = -\frac{s}{|s|}\left\{\frac{\rho^2}{2}\left[(F'_{\rm m}(\lambda\rho))^2 - F_{\rm m}(\lambda\rho) F''_{\rm m}(\lambda\rho) - \frac{1}{\lambda\rho} F_{\rm m}(\lambda\rho) F'_{\rm m}(\lambda\rho)\right]\right\}\Big|_{R_1}^{R_2}. \tag{A.5}$$

Now, in terms of ξ variable, (A.4) can be put into the form:

$$|a_{mq}^{(1)}|^{-2} = \frac{\xi}{2}\left(\frac{1}{g_\perp^2} + \frac{s}{g_\parallel^2}\right) F'_{\rm m}(\xi) F_{\rm m}(\xi)\Big|_{R_1}^{R_2} + \frac{\xi^2}{2}\left(\frac{1}{g_\perp^2} - \frac{s}{g_\parallel^2}\right)\left[(F'_{\rm m}(\xi))^2 - F_{\rm m}(\xi) F''_{\rm m}(\xi)\right]\Big|_{R_1}^{R_2}, \tag{A.6}$$

where $\xi_{1,2} = \lambda R_{1,2}$.

By taking into account the relations:

$$\frac{1}{g_{\parallel,\perp}^2(\omega)} = \frac{\varepsilon_0}{2\omega}\frac{\partial\varepsilon_{\parallel,\perp}(\omega)}{\partial\omega}, \tag{A.7}$$

and

$$\frac{\partial\xi}{\partial\omega} = \frac{\xi}{2\varepsilon_\parallel\varepsilon_\perp}\left(\varepsilon_\perp\frac{\partial\varepsilon_\parallel}{\partial\omega} - \varepsilon_\parallel\frac{\partial\varepsilon_\perp}{\partial\omega}\right), \tag{A.8}$$

(A.6) can be put into the form

$$|a_{mq}^{(1)}|^{-2} = \frac{\varepsilon_0}{4\omega\varepsilon_\parallel}(I(R_2) - I(R_1)). \tag{A.9}$$

In the above expression we have denoted

$$I(\rho) = \frac{\partial}{\partial\omega}(\varepsilon_\parallel\varepsilon_\perp)\xi F'_{\rm m}(\xi,\omega) F_{\rm m}(\xi,\omega) - 2(\varepsilon_\parallel\varepsilon_\perp)\xi \times \frac{\partial\xi}{\partial\omega}\left[(F'_{\rm m}(\xi,\omega))^2 - F_{\rm m}(\xi,\omega) F''_{\rm m}(\xi,\omega)\right]. \tag{A.10}$$

At this moment, we have to stress that in (A.10) the function $F_{\rm m}(\xi,\omega)$ depends on R_1 due to electrostatic boundary conditions at the inner surface, a fact which leads to the dependence on R_1 of the coefficients $\alpha_{mq}(\omega)$ and $\beta_{mq}(\omega)$. Because, at the two surfaces, the electrostatic boundary conditions are written in terms of the functions

$$g^{(1,2)}(\omega) = \frac{F_{\rm m}(\xi_{1,2},\omega)}{F'_{\rm m}(\xi_{1,2},\omega)}, \tag{A.11}$$

in the following, we shall evaluate the ω derivative for these functions, by taking into account the double dependence on ω as we have mentioned before. Now, performing the ω derivative of the functions defined by (A.11), and taking into account the expression (14) of the Wronskian, one obtains

$$\frac{\partial g^{(i)}(\omega)}{\partial\omega} = \frac{\partial\xi_i}{\partial\omega}\left[1 - \frac{F_{\rm m}(\xi_i,\omega) F''_{\rm m}(\xi_i,\omega)}{(F'_{\rm m}(\xi_i,\omega))^2}\right] + \frac{1}{\xi_i}\frac{s}{|s|}\left(\alpha_{mq}(\omega)\frac{\partial\beta_{mq}(\omega)}{\partial\omega} - \beta_{mq}(\omega)\frac{\partial\alpha_{mq}(\omega)}{\partial\omega}\right) \times \frac{1}{(F'_{\rm m}(\xi_i,\omega))^2} \tag{A.12}$$

with $i = 1, 2$.

In these conditions, (A.9) becomes

$$|a_{mq}^{(1)}|^{-2} = \frac{\varepsilon_0}{4\omega}\frac{\xi_2}{\varepsilon_\parallel}(F'_{\rm m}(\xi_2,\omega))^2\left\{\frac{\partial}{\partial\omega}(\varepsilon_\parallel\varepsilon_\perp) g^{(2)}(\omega) - 2\varepsilon_\parallel\varepsilon_\perp\frac{\partial g^{(2)}(\omega)}{\partial\omega}\right\} - \frac{\varepsilon_0}{4\omega}\frac{\xi_1}{\varepsilon_\parallel}(F'_{\rm m}(\xi_1,\omega))^2 \times \left\{\frac{\partial}{\partial\omega}(\varepsilon_\parallel\varepsilon_\perp) g^{(1)}(\omega) - 2\varepsilon_\parallel\varepsilon_\perp\frac{\partial g^{(1)}(\omega)}{\partial\omega}\right\}, \tag{A.13}$$

an expression which, after some calculations, can be transformed into a more compact form:

$$|a_{mq}^{(1)}|^{-2} = -\frac{\varepsilon_0}{2\omega}|q|R_2|\varepsilon_\parallel(\omega)\varepsilon_\perp(\omega)|(F'_{\rm m}(\xi_2,\omega))^2 \times \frac{\partial}{\partial\omega}\left(\frac{\sqrt{|s(\omega)|}}{\varepsilon_\perp(\omega)} g^{(2)}(\omega)\right) + \frac{\varepsilon_0}{2\omega}|q|R_1|\varepsilon_\parallel(\omega)\varepsilon_\perp(\omega)|(F'_{\rm m}(\xi_1,\omega))^2 \times \frac{\partial}{\partial\omega}\left(\frac{\sqrt{|s(\omega)|}}{\varepsilon_\perp(\omega)} g^{(1)}(\omega)\right). \tag{A.14}$$

From the electrostatic boundary conditions (12) and (13) at the surface $\rho = R_1$, the following relation results:

$$g^{(1)}(\omega)\frac{\sqrt{|s(\omega)|}}{\varepsilon_\perp(\omega)} = \frac{I_{|m|}(|q|R_1)}{I'_{|m|}(|q|R_1)}, \tag{A.15}$$

which leads to

$$\frac{\partial}{\partial\omega}\left(g^{(1)}(\omega)\frac{\sqrt{|s(\omega)|}}{\varepsilon_\perp(\omega)}\right) = 0. \tag{A.16}$$

Consequently, the second term of the expression (A.14) cancels. In these conditions, the form of the normalization constant of the eigenvectors of the optical phonon field can be written in terms of the ω derivative of the function $f_{\rm m}(q,\omega)$ defined in (20), obtaining

$$|a_{mq}|^{-2} = \frac{\varepsilon_0}{2}|q|R_2\left[|\varepsilon_\parallel(\omega)\varepsilon_\perp(\omega)|\left(F'_{\rm m}\left(\frac{|q|R_2}{\sqrt{|s(\omega)|}},\omega\right)\right)^2 \times \frac{1}{\omega}\frac{\partial f_{\rm m}(q,\omega)}{\partial\omega}\right]_{\omega=\omega_{\rm ml}^{(\mu)}(q)}. \tag{A.17}$$

We have chosen this approach to derive the expression of the normalization constant because it readily yields a generalization to the case of the core–shell structure of the type GaN/AlN, for example.

It is important to verify that, in the limit of a quantum wire ($R_1 \to 0$, $R_2 = R$) the expression (A.17) recovers the relation (B.10) in [16]; for the sake of simplicity we shall restrict ourselves to the particular case of the surface phonon modes. Thus, for the surface modes of a wire, the dispersion laws are given by the relation (22) in [16]:

$$f_{mq}^{(0)} = 0, \qquad \text{with}$$

$$f_{mq}^{(0)} = \frac{\varepsilon_\perp(\omega)}{\sqrt{s(\omega)}} - \frac{I_{|m|}\left(\frac{|q|R}{\sqrt{s(\omega)}}\right) K'_{\mathrm{m}}(|q|R)}{I'_{|m|}\left(\frac{|q|R}{\sqrt{s(\omega)}}\right) K_{\mathrm{m}}(|q|R)}. \tag{A.18}$$

In the limit $R_1 \to 0$, $R_2 = R$, the function $F_{\mathrm{m}}(\frac{|q|R}{\sqrt{|s(\omega)|}})$ becomes the modified Bessel function of first kind $I_{|m|}(\frac{|q|R}{\sqrt{|s(\omega)|}})$ so that, in this particular case, the functions $f_{mq}^{(0)}(\omega)$ and $f_{\mathrm{m}}(q, \omega)$ are related by the following expression:

$$f_{\mathrm{m}}(q, \omega) = -\frac{K_{\mathrm{m}}(|q|R)}{K'_{\mathrm{m}}(|q|R)} \frac{f_{mq}^{(0)}(\omega)}{\sqrt{\varepsilon_\perp(\omega)\varepsilon_\parallel(\omega)}}. \tag{A.19}$$

Because, both (20) and (A.18) have the same solutions (the frequencies of the surface phonon modes), denoted here, for the sake of simplicity, by $\tilde{\omega}$, it is easily verified that

$$\left(\frac{\partial f_{\mathrm{m}}(q, \omega)}{\partial \omega}\right)\Bigg|_{\omega=\tilde{\omega}} = \frac{1}{\varepsilon_\perp(\omega)\varepsilon_\parallel(\omega)} \frac{I_{|m|}\left(\frac{|q|R}{\sqrt{s(\omega)}}\right)}{I'_{|m|}\left(\frac{|q|R}{\sqrt{s(\omega)}}\right)} \frac{\partial f_{mq}^{(0)}}{\partial \omega}\Bigg|_{\omega=\tilde{\omega}}, \tag{A.20}$$

proving that (A.17) reduces to the expression (B.10) in [16].

References

[1] Iijima S 1991 *Nature* **354** 56
[2] Tazlaoanu C, Ion L, Enculescu I, Sima M, Enculescu M, Matei E, Neumann R, Bazavan R, Bazavan D and Antohe S 2008 *Physica* E **40** 2504
[3] Goldberger J, He R R, Zhang Y F, Lee S W, Yan H Q, Choi H J and Yang P D 2003 *Nature* **422** 599
[4] Hung S-C, Su Y-K, Chang S-J and Chen Y H 2006 *Microelectron. Eng.* **83** 2441
[5] Wu Q, Hu Z, Wang X Z, Lu Y N, Chen X, Xu H and Chen Y 2003 *J. Am. Chem. Soc.* **125** 10176
[6] Balasubramanian C, Bellucci S, Castrucci P, De Crescenzi M and Bhoraskar S V 2004 *Chem. Phys. Lett.* **383** 188
[7] Bengu E and Marks L D 2001 *Phys. Rev. Lett.* **86** 2385
[8] Loudon R 1964 *Adv. Phys.* **13** 423
[9] Chamberlain M P, Cardona M and Ridley B K 1993 *Phys. Rev.* B **48** 14356
[10] Chang Y-M and Chang N-A 2003 *J. Appl. Phys.* **93** 2015
[11] Zhang L and Shi J J 2005 *Semicond. Sci. Technol.* **20** 592
[12] Zhang L, Shi J J and Tansley T L 2005 *Phys. Rev.* B **71** 245324
[13] Zhang L and Shi J J 2006 *Phys. Status Solidi* b **243** 1775
[14] Merten L 1972 *Atomic Structure and Properties of Solids* (New York: Academic)
[15] Gray A and Mathews G B 1922 *A Treatise on Bessel Functions and Their Applications to Physics* (London: MacMillan)
[16] Brancus D E N and Ion L 2007 *Phys. Rev.* B **76** 155304
[17] Harima H 2002 *J. Phys.: Condens. Matter* **14** R967
[18] Brancus D E N and Mocuta A C 1995 *Can. J. Phys.* **73** 126
[19] Racec E R and Brancus D E N 1998 *J. Phys.: Condens. Matter* **10** 3845